Original Research

Investigation of the adsorptive capacity of a poly(vinyl alcohol)-based film for sodium diclofenac in aqueous media

Juliana Zanol Merck* (ORCID)
Camila Suliani Raota (ORCID)
Jocelei Duarte (ORCID)
Camila Baldasso (ORCID)
Marcelo Giovanela (ORCID)
Janaina da Silva Crespo* (ORCID)

Universidade de Caxias do Sul, Área do Conhecimento de Ciências Exatas e Engenharias, Rua Francisco Getúlio Vargas, 1130, Caxias do Sul 95070-560, Brazil.
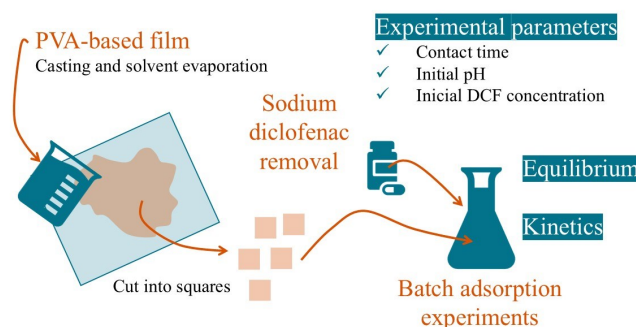*Corresponding author: jzmerck@ucs.br (JZM); jscrespo@ucs.br (JSC).

Abstract: Sodium diclofenac (DCF) has been detected in waters worldwide and is considered a micropollutant of emerging concern due to its potential toxicity in aquatic and terrestrial ecosystems. Traditional water treatment methods are unable to remove DCF completely from water, which makes adsorptive films a suitable alternative to address this challenge. In this context, the present study investigated the adsorptive capacities of a poly(vinyl alcohol)-based film for removing DCF from aqueous solutions. The effects of the initial DCF concentration and solution pH on the adsorption performance were evaluated, as well as kinetics and equilibrium isotherms. Regarding the results, DCF precipitation was observed within a pH range of 4.0-7.0, probably due to its limited solubility in acidic media. The optimal DCF concentration was found to be the lowest tested (2.5 mg L^{-1}), yielding an equilibrium adsorption capacity (q_e) of 0.511 mg g^{-1} and a DCF removal percentage (*%R*) of 23.4% within 90 min. Although the adsorption equilibrium was well described by the Redlich-Peterson isotherm despite the unusual behavior observed, pseudo-first and pseudo-second order kinetic models were satisfactory only at the initial concentration of 2.5 mg L^{-1}. Overall, the data set indicate that the film has a limited adsorption capacity, reaching saturation at low adsorbate concentrations. Nonetheless, these findings support further investigations at lower DCF concentrations to better understand the film's adsorptive behavior under environmentally relevant conditions.

Keywords: Poly(vinyl alcohol), citric acid, crosslinked film, sodium diclofenac, adsorption, isotherms, kinetics.

Introduction

The increasing water scarcity concerns scientists and authorities worldwide [1], and relates to the growth of the human population and emerging new forms of water contamination. Some examples are emergent organic micropollutants, such as pesticides, pharmaceuticals, and personal hygiene products [2, 3]. Besides bringing harmful environmental effects even at trace concentrations, their removal at conventional water treatment systems is also challenging [3].

Non-steroidal anti-inflammatory drugs (NSAIDs), commonly consumed by humans and animals, have been detected in various environmental compartments, including surface water, groundwater, and soils [4]. NSAIDs and other pharmaceuticals reach water bodies through contaminated wastewater, considering that between 40 and 90% of the ingested dose leaves the body in its unalerted form or a biologically active metabolite [3]. Among this class of medicines, sodium diclofenac (DCF) stands out for its analgesic, antipyretic, and anti-inflammatory properties. However, this drug has already proven adverse effects on aquatic and terrestrial ecosystems [4].

As described by Lonappan *et al.* [4], DCF concentrations at ng L^{-1} level may cause chronic effects on fish, such as delay in egg hatching. Additionally, the drug may accumulate in gills, muscle, liver, and kidney tissues, causing cytological abnormalities. Mussel species might have their metabolism, growth, and tissues affected. According to Eades and Waring [5], DCF exposure is also prejudicial to crabs of the *Carcinus maenas* species, altering their osmoregulation capacity.

To mitigate further contamination, effective removal techniques are required. Biological treatments are the most widely used in wastewater treatment due to the relatively low costs, high removal rates of organic matter, and capability to handle large volumes [6]. Activated sludge processes are commonly used in wastewater treatment [7], especially in the pharmaceutical industry [8]. They consist of the degradation of pollutants into acceptable forms or conversion into water and carbon dioxide through mineralization, using microorganisms. In this case, removal occurs by biotransformation, sorption onto sludge, and phototransformation [7].

DCF exhibits a low water-sludge distribution coefficient, indicating a higher prevalence in the liquid phase [7], being less likely adsorbed onto sludge. The photodegradation caused by sunlight eliminates approximately 90% of DCF in lakes. Nevertheless, certain degradation by-products of DCF can increase toxicity by up to sixfold. Moreover, the complexes of DCF and Hg (II), Pb (II), and Sn (II) ions present antimicrobial activity whose effects on biological treatment remain incompletely understood [4].

The review published by Zhang *et al.* [7] reports the DCF removal efficiency of various biological treatment approaches, including conventional activated sludge processes, membrane reactors, and sequencing batch reactors. The removal rates were up to 80%, with a more common range between 21 and 40%. Alternative processes have been studied to improve these rates, such as the non-conventional techniques of pressure-driven membrane processes and adsorption [9, 10].

Membrane separation processes stand out for their compacity, stability, and satisfactory performance [10]. Regarding DCF removal from aqueous media, reverse osmosis laboratory-scale studies have reported removal rates exceeding 98% [11]. Additionally, adsorption has emerged as a superior alternative to conventional wastewater treatment methods due to its low energy consumption, ease of operation, and high efficiency [12, 13]. From an environmental perspective, adsorption is an interesting alternative as the solid residues generated are limited compared to flocculation and coagulation processes, which produce sludge [12]. The possibility of regenerating and reusing the adsorbent also contributes to operational cost reduction, even though final disposal might be challenging [14].

Another promising technology involves integrating adsorption and membrane processes for micropollutant removal. The adsorptive membranes offer several advantages, including high removal rates and efficiency, high permeate flux, low operation pressure, regeneration, and reusability. For this purpose, materials with adsorptive capabilities are incorporated into the membrane, aiming to overcome drawbacks associated with both processes when applied separately. The fillers can be organic, inorganic, or biomaterials, and there are several preparation techniques to incorporate them into the membrane polymer matrix [1].

This technology has not been widely studied for the removal of pharmaceuticals from water, though it shows potential [15]. For example, Raicopol *et al.* [16] have developed cellulose acetate membranes with layered double hydroxides (LDHs) to increase adsorption capacity and permeability. The membrane with 4% (*w/w*) Mg-Al LDHs showed a remarkable tenfold increase in DCF adsorption capacity compared to pristine cellulose acetate membranes and exhibited higher water flux.

Poly(vinyl alcohol) (PVA) is a fossil-based synthetic polymer known for its outstanding hydrophilicity, which arises from the presence of hydroxyl groups in its structure. Additionally, it is biodegradable, nontoxic, and well-suited to film formation [17, 18]. Consequently, studies have been exploring its potential applications in water treatment, including membrane separation processes and adsorption for removing contaminants, such as dyes [19] and pharmaceuticals [20]. In alignment with eco-friendly approaches, PVA serves as a polymer adsorbent that offers structural diversity and tunable physicochemical properties [21]. Furthermore, adsorptive films made from PVA can be more easily prepared, applied, and recovered compared to conventional adsorbents [12].

In this context, Raota *et al.* [22] produced a green PVA-based membrane crosslinked with citric acid, containing glycerol and green synthesized silver nanoparticles (AgNPs) for DCF removal. Besides the membrane performance comparable to loose nanofiltration commercial membranes (44% of DCF removal at 3 bar, with 2.2 L m^{-2} h^{-1} of permeate flux), the authors hypothesized a combined rejection and adsorption of DCF by the membrane. A subsequent work [23] demonstrated that the membrane has adsorptive capacity for DCF removal through batch adsorption experiments. However, better comprehension of the membrane's adsorptive behavior still requires deeper investigations.

In light of these considerations, this study aimed to investigate the DCF adsorptive capacity of the referred PVA-based membrane through batch adsorption experiments. Since the selective capacity of the membrane was not evaluated, it will be referred to as *"film"* throughout this work. The effects of contact time, initial DCF concentration, and initial pH of the media on the film's adsorptive performance were examined, and adjustments to equilibrium and kinetic models were also performed.

Experimental Section

Chemicals and materials

The high-purity DCF (≥ 98%) and PVA (M_W of 85,000-124,000 kDa, degree of hydrolysis > 99%) were acquired from Sigma-Aldrich (Brazil). Glycerol (propane-1,2,3-triol) and ethanol (95%) were purchased from Vetec Química Fina Ltda. (Brazil). Anhydrous citric acid (2-hydroxy-1,2,3-propanetricarboxylic acid, analytical grade) was obtained from Cinética Ltda. (Brazil), and silver nitrate (≥ 99%) from Merck (Brazil). Distilled water for solution preparation was produced using a Pilsen distiller (Quimis, model Q341-210). pH adjustments were performed by adding small quantities of HCl and NaOH aqueous solutions (0.1 mol L^{-1}) prepared from commercial chemicals NaOH 98-100% and HCl 37-38%

(Merck Brazil). The resulting pH was monitored using a pH meter (MS Tecnopon, model mPA-210).

According to a previous study [24], the AgNPs were synthesized using a green synthesis approach. Briefly, an aqueous solution of AgNO$_3$ (2.5 mmol L^{-1}) was combined with an equal volume of hydroalcoholic grape pomace extract (50 g L^{-1}, pH = 10.0) at room temperature, yielding an AgNP solution with a final concentration of 1.25 mmol L^{-1}.

Preparation of the PVA-based films

The films were fabricated using the casting and solvent evaporation method, as outlined in our previous work [22]. Initially, PVA was dissolved in distilled water at 80 °C (heated bath, VEB MLW, model U2C) under stirring (Velp Scientifica, model ARE) for 24 h to obtain a 10% (*w/v*) solution.

The film solution was prepared by combining 32 mL of the PVA solution with 0.32 g of citric acid and 1.6 g of glycerol, and the mixture was stirred for 30 min at 50 °C. Subsequently, 8,0 mL of an AgNP solution was added, and the mixture was stirred for additional 5 min. Any bubbles were eliminated using an ultrasonic bath (Unique, model USC-1400A) for 30 min.

Later, 40 mL of the resulting mixture was poured and spread onto a glass plate (~1.0 mm, wet thickness), and left to dry at room temperature (23 °C) for 24 h. The films were carefully removed from the plates and went through a heat treatment (110 °C, 110 min) in an air circulation oven (DeLeo, model AGSEDT). Finally, the films were stored at room temperature until they were used in the experiments.

These films have been also characterized in our previous work [22], regarding their morphology, chemical, and physical properties, as well as their performance in filtration experiments. The relevant characterization results will be highlighted in the Results section to improve the quality of the discussion.

Batch adsorption experiments

For the batch adsorption experiments, the films are precisely cut into 1.0 cm² squares. Hereafter, the films were also referred to as *"adsorbent"*. A specific mass of the adsorbent was added into Erlenmeyer flasks containing 50 mL of a DCF aqueous solution. Then, the experiments were conducted in a refrigerated incubator shaker (Novatécnica, model NT-715) set to 25 °C with stirring frequency of 240 rpm.

At the end of each experiment, a solution sample was collected to determine the DCF concentration using ultraviolet-visible (UV-Vis) spectroscopy with a Beckman Coulter spectrophotometer (model DU-530). The absorbance was recorded at 274 nm [25], and the concentration was determined using an equation derived from linear regression based on a calibration curve prepared in distilled water, ranging from 1.0 to 30.0 mg L^{-1}.

The film adsorptive performance was assessed using adsorption capacity (*q(t),* mg g^{-1}) and removal percentage (*%R, %*), using Equations (1) and (2), respectively:

$$q(t) = \frac{[C_0 - C(t)] \cdot V}{m} \tag{1}$$

$$\%R = \frac{[C_0 - C(t)]}{C_0} \cdot 100\% \tag{2}$$

where, C_0 and $C(t)$ represent, respectively, the DCF concentrations (mg L^{-1}) at the initial conditions ($t = 0$) and at time t, m is the mass of adsorbent (g), and V is the volume of DCF solution (L).

Considering the lack of information regarding the performance of PVA-based films in adsorption, a preliminary investigation was conducted to elucidate the material behavior and establish initial experimental conditions. The experimental conditions explored at this stage are detailed in Table 1. The mass of the adsorbent (50 and 500 mg, corresponding to 6.0 and 60.0 cm², respectively) and contact time (from 240 to 360 min) were evaluated at the initial DCF concentration of 10 mg L^{-1}, using the natural solution pH (pH ~ 5.75). The glassware washing procedures (see in Glassware washing section) are also specified for each experiment in Table 1. The conditions yielding the most favorable adsorbent performance were employed in the subsequent experiments.

Table 1. Preliminary adsorption experiments for understanding the DCF adsorption behavior using the PVA-based film.

Experiment [a]	Mass of adsorbent (mg)	Maximum contact time (min)	Glassware washing procedure
M500T240E	500	240	Extran®
M500T360E	500	360	Extran®
M500T360N	500	360	Neutral detergent
M50T240N	50	240	Neutral detergent

[a] Experiment coding: the number preceded by the letter "M" indicates the mass of adsorbent, while the number preceded by "T" indicates the contact time; the letters "E" and "N" refer to the glassware washing procedure applied (Extran® and neutral detergent, respectively).

Additionally, blank experiments were conducted using flasks representative of each washing procedure to ascertain the presence of contaminants and interferers. In these experiments, the DCF solution was substituted with distilled water, no adsorbent was used, and all other conditions (stirring frequency, temperature, and volume) were consistent with the main experiments.

Glassware washing

The first glassware washing method involved washing with tap water, immersion in alkaline Extran® (5% *v/v*) for at least 24 h, rinsing with tap water, and air drying at room temperature. It was replaced due to interference in the UV-Vis analysis, as indicated by results from the blank samples (Section 2, Supplementary Material). For the second procedure,

the flasks were washed with tap water and neutral detergent, followed by vigorously rinsing with tap water, and dried overnight in an oven at 80 °C.

Film characterization by UV-Vis spectroscopy

The film was characterized using UV-Vis spectroscopy to assess its characteristic absorbance and identify potential interferences in the DCF quantification method, as discussed previously (see Preliminary adsorption experiments section). The spectrum was obtained using a spectrophotometer (DU530, Beckman, Indianapolis, IN, USA) over a wavelength range of 200 to 690 nm, with a resolution of 1.0 nm. The film was pinned onto the sample holder and positioned within the light beam for analysis.

Effect of experimental conditions in batch adsorption experiments

Contact time (minimum interval for attaining equilibrium) was optimized in the preliminary experiments (see Batch adsorption experiments section), and employed for optimizing the initial pH and concentration of DCF solution. The effect of initial pH was examined by conducting experiments at pH levels of 4.0, 5.0, 7.0, 8.0, and 9.0. The other experimental conditions remained constant, including a contact time of 240 min, a mass of adsorbent of 50 mg, and an initial DCF concentration of approximately 10 mg L^{-1}.

Subsequently, the initial DCF concentration was varied (2.5, 5.0, 8.5, 10.0, and 15.0 mg L^{-1}) using the previously optimized conditions. At this stage, experiments with progressively longer contact times (up to 360 min) were also performed to evaluate the adsorption kinetics until equilibrium.

Evaluation of equilibrium and kinetics of the adsorption process

For the construction of the isotherms, the DCF equilibrium concentration (C_e) was calculated as the arithmetic mean of the last two concentrations measured during the equilibrium (between 60 and 90 min) for initial concentrations ranging from 2.5 to 10.0 mg L^{-1}. Then, the adsorption capacity at equilibrium (q_e) was calculated using Equation (1). The experimental data were then correlated with Langmuir, Freundlich, Temkin, Sips, and Redlich-Peterson models, as well as the pseudo-first (PFO) and pseudo-second order (PSO) kinetic models (Section 1, Supplementary Material).

The parameters for both isotherm and kinetic adjustments were obtained using the Microsoft Excel Solver function, with the objective set as the minimum mean square error between the experimental data and the calculated values of q_e and $q(t)$ [26]. The mean square error (used as the objective function, OF) was calculated according to Equation (3), where EP represents the number of experimental points, and $q_{i,\,exp}$ and $q_{i,\,calc}$ denote, respectively, the experimentally obtained adsorption capacity and the calculated adsorption capacity:

$$OF = \frac{1}{EP} \cdot \sum_{i=1}^{EP} (q_{i,\,exp} - q_{i,\,calc})^2 \qquad (3)$$

In addition to the OF values, the correlations between models and experimental values were assessed using the coefficient of determination (R^2), as defined in Equation (4):

$$R^2 = 1 - \frac{\sum (q_{exp} - q_{calc})^2}{\sum (q_{exp} - q_{med})^2} \qquad (4)$$

where, q_{exp} corresponds to the experimental values for adsorption capacity, q_{calc} represents the calculated adsorption capacity, and q_{med} is the mean value of the experimentally obtained adsorption capacities.

Results and Discussion

Preliminary adsorption experiments

Figure 1 shows the (A) adsorption capacity and (B) DCF removal as a function of contact time for the preliminary experiments. The adsorption capacity of M500T240E increased rapidly at the initial contact time followed by a trend towards equilibrium. Consequently, the contact time was extended to 360 min in the subsequent experiment (M500T360E). However, the results diverged significantly compared to M500T240E. Some interferent might have caused the instability observed. The results from blank experiments (Table S2, Supplementary Material) characterize Extran® residues as sources of interference.

After adjusting the glassware cleaning protocol, the experiment M500T360E was repeated (M500T360N in Figure 1). The observed pronounced evolution followed by the establishment of equilibrium at 240 min was considerably similar to the results reported for M500T240E. As an attempt to observe a more gradual evolution at the initial time intervals, the mass of the adsorbent was reduced to 50 mg (M50T240N). For that experiment, the $q(t)$ increased more gradually in the early stages, although some instability persisted. Furthermore, the adsorption performance did not suffer significant variation with the tenfold mass reduction. Consequently, the removal percentage decreased drastically, as shown in Figure 1B.

The performance drop at the end of contact time for M500T360N and M50T240N is another unexpected result, attributed to some interferent released by the film during the experiment, which might absorb the wavelengths within the UV region. The film UV-Vis spectrum (Figure S1, Supplementary Material) reveals a peak at 288 nm (considerably close to 274 nm, the wavelength used in DCF quantification), which might be related to residual acetate groups and non-crosslinked citric acid. Due to the PVA synthetic route (hydrolysis of poly(vinyl acetate)), residual acetate groups remain in the final polymer, allowing electronic transitions associated with absorption at 280-335 and 282-327 nm [27, 28]. However, the FTIR spectrum of the pure PVA used to prepare the films did not display the characteristic bands associated with residual acetate (C–O and C=O stretching, at approximately 1020 and 1700 cm^{-1}, respectively), [23].
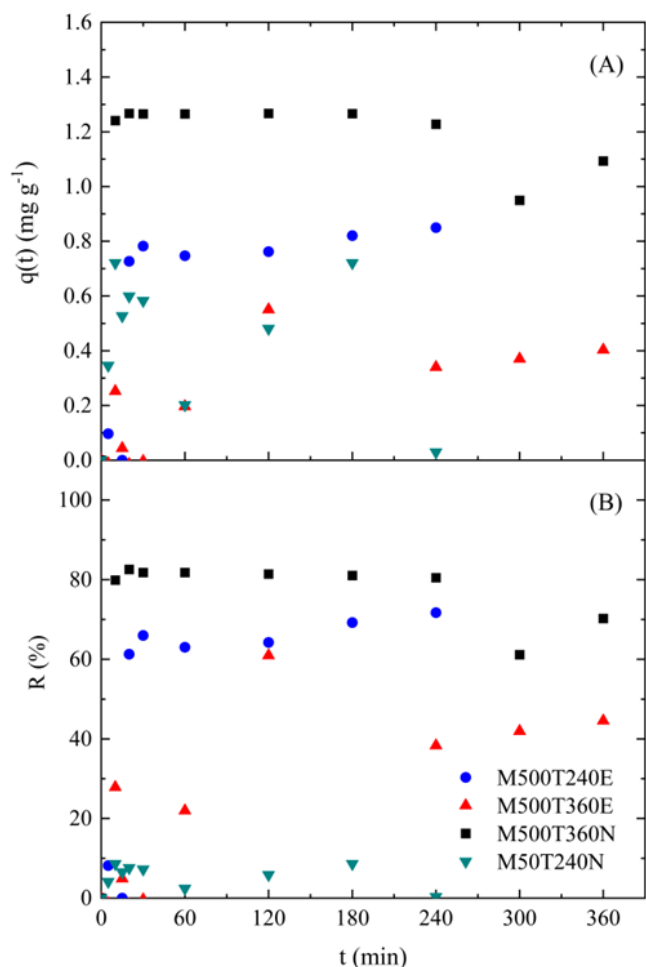
Figure 1. (A) Adsorption capacity and (B) DCF removal as a function of time for the preliminary experiments. Experimental conditions: 25 °C, 240 rpm, 50 mL initial adsorbate solution volume, pH ~ 5.75, DCF initial concentration of 10.0 mg L^{-1}.

This absence may be attributed to the high degree of hydrolysis (> 99%), although highly hydrolyzed PVA can still exhibit residual acetate FTIR vibrations [29].

Therefore, there is insufficient evidence to rule out the possible influence of these groups. Additionally, citric acid has three carboxyl groups that absorb within the same ultraviolet region. Krishnaswamy *et al.* [30] observed a peak at 282 nm in a commercial citric acid spectrum, while Mohan *et al.* [31] identified a peak at 230 nm in a lemon juice spectrum, both associated with the presence of this carboxylic acid.

For the subsequent experiments, the mass of adsorbent was set at 50 mg, since the reduction from 500 to 50 mg did not significantly diminish adsorptive performance (from 1.266 to 0.721 mg g^{-1}). A 240 min contact time was chosen as the equilibrium could be achieved within this timeframe. Furthermore, the presence of Extran® was shown to interfere negatively with adsorbent performance, thus the glassware cleaning protocol was changed. Within the initial conditions defined, the effect of pH on the film adsorptive behavior was subsequently assessed.

Effect of DCF solution initial pH in the film adsorption performance

The adsorption capacity and removal percentage at the different pH values are presented in Figure 2. The best performance was obtained at pH = 4.15, though the presence of precipitate suggested that the DCF solubility had been affected.
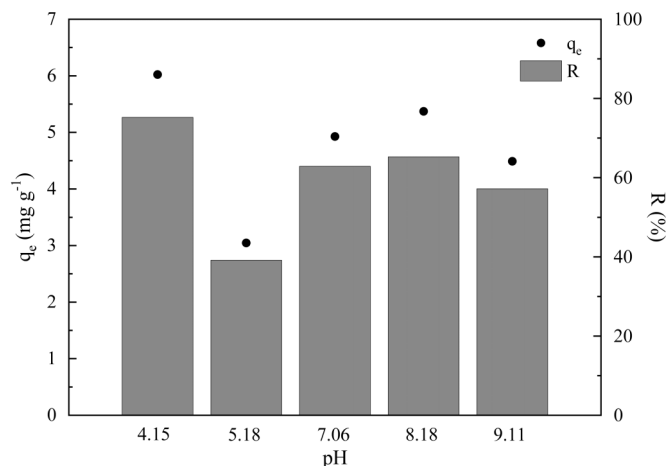

Figure 2. Effect of initial pH over adsorption capacity and DCF removal using the PVA-based film. Experimental conditions: 25 °C, 240 rpm, initial adsorbate solution volume of 50 mL, initial DCF concentration of 10 mg L^{-1}, contact time of 240 min.

As a weak acid (pK_a = 4.0), DCF solubility is strongly influenced by the pH of the medium. At pH below 4.0, the protonated form (less soluble) prevails. Conversely, at pH values above the pK_a of DCF, the predominant form is dissociated, resulting in a negative charge molecule [12]. Precipitation was identified within the initial pH range from 4.15 to 7.06, suggesting the film likely altered the solution pH closer to the pK_a of DCF during the experiment.

To investigate that behavior, the final pH of every sample was measured, and the pH variation (ΔpH) could be calculated (Table S3, Supplementary Material). Despite the initial value, the final pH of all samples decreased, approaching 4.0. Additionally, the plot of pH variation as a function of initial pH (Figure S2, Supplementary Material) shows a linear increase of ΔpH with increasing initial pH.

Using a linear regression analysis, the initial pH value that would not cause a pH variation (ΔpH = 0) occurs at 4.05, within the range of reduced DCF solubility (from 1.2 to 3.6 mg L^{-1} between pH 1.0 and 4.5) [32]. Consequently, precipitation is anticipated for DCF concentrations exceeding the solubility limit. The film's point of zero charge (pH_{PZC}), as determined by Raota *et al.* (2024) [23], is 3.88, which is close to the estimated value of 4.05. Thus, the film surface would be negatively charged at superior pH values. As deprotonated DCF is also negatively charged, an electrostatic repulsion would occur between the drug and the film, leading to reversible adsorption [33].

The initial pH of 8.0 was determined as the optimized condition, since it yielded relatively favorable results

concerning q_e and $\%R$ (5.37 mg g^{-1} and 65.3%, respectively), also ensuring a final pH farthest from pK_a of DCF (4.30).

Effect of DCF solution initial concentration in the film adsorption performance

Figure 3 presents the adsorption capacity and removal percentage as a function of time for the evaluated initial DCF concentrations. The results from 2.5 to 10.0 mg L^{-1} were notably similar, whereas the performance at 15.0 mg L^{-1} is at a higher range (Figure 3A). The lower concentrations reached equilibrium within 60-90 min, with the best results at 2.5 mg L^{-1} (q_e = 0.511 mg g^{-1}). The q_e values for 5.0, 8.5, and 10.0 mg L^{-1} were 0.246, 0.202, and 0.206 mg g^{-1}, respectively. Despite the increase in initial DCF concentration, the film maintained consistent performance (Figure 3B), which led to the decline in removal percentage: 23.4, 6.6, 2.6, and 3.0% for 2.5, 5.0, 8.5, and 10.0 mg L^{-1}, respectively.

For conventional adsorbents, an increase in adsorption capacity is expected when enhancing initial adsorbate concentration, due to intensifying concentration gradient between the solid surface and the media [12, 25]. The
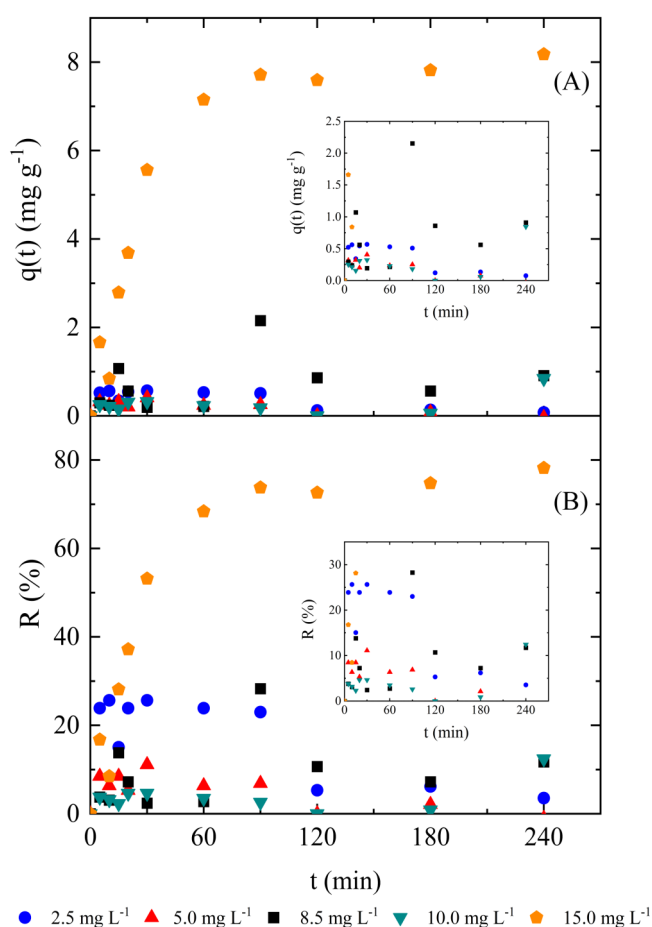
contrary is observed for the PVA-based film, which could relate to the dense film's characteristics [22], restricting the availability of adsorption sites. Hence, less adsorbate might be sufficient to cause saturation. Additionally, at lower concentrations, the ratio between DCF and the available film sites is reduced, resulting in more available adsorption sites compared to higher adsorbate concentrations [34].

At 15.0 mg L^{-1}, equilibrium was reached in 90 min, yielding q_e = 7.997 mg g^{-1} and $\%R$ = 76.5%. However, precipitation occurred due to DCF concentration exceeding the drug solubility limit (3.6 mg L^{-1}), mirroring observations from the pH experiments. Consequently, it is not possible to distinguish between adsorption and precipitation in the overall removal of DCF. Therefore, these results were not considered for equilibrium and kinetics evaluation.

No precipitation was observed for the other concentrations (2.5-10.0 mg L^{-1}) even though the solubility limit had been transcended above 5.0 mg L^{-1}. Thus, precipitation could have occurred although not visually identified. The concentration of 2.5 mg L^{-1} was the only one below the DCF solubility limit Consequently, removal at this condition was most likely due to adsorption.

Adsorption equilibrium

Figure 4 illustrates the fitting of the adsorption capacity at equilibrium as a function of DCF equilibrium concentration for the isotherm models tested. Most adjustments do not correlate well with the experimental data, which may be attributed to the unusual adsorption behavior: q_e drops from 2.5 to 5.0 mg L^{-1}, followed by a tendency to stabilize above 8.5 mg L^{-1}. The parameters obtained for each isotherm equation tested are presented in Table S4 (Supplementary Material).

Overall, the Redlich-Peterson model exhibited the lowest OF value (7.748 × 10^{-4}) and the R^2 closest to unity (0.9767), Moreover, it was the only model that adequately represented

Figure 3. (A) Adsorption capacity and (B) DCF removal as a function of time for the studied initial DCF concentrations in the solution. Experimental conditions: 25 °C, 240 rpm, initial adsorbate solution volume of 50 mL, initial pH ~ 8.0.
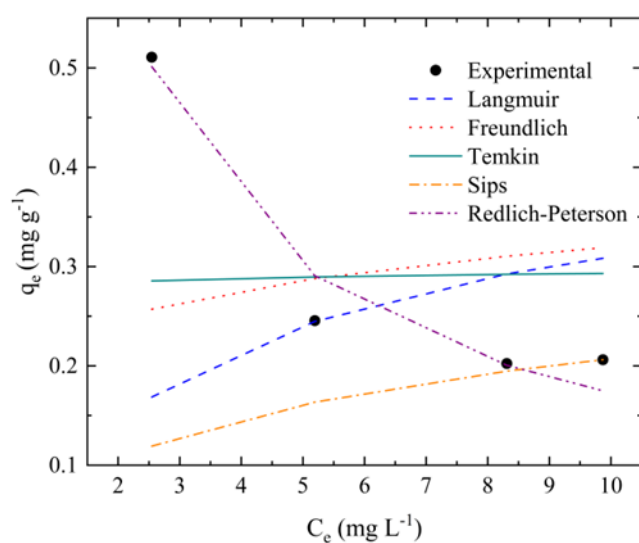

Figure 4. Adsorption capacity of the PVA-based film at equilibrium as a function of the DCF equilibrium concentration, along with the adjustments for the isotherm models.

the unusual decreasing behavior of q_e. Additionally, the Redlich-Peterson exponential constant obtained $\beta RP = 1.800$ (see Table S4 in Supplementary Material) exceeds the interval of 0-1, where the model would typically indicate a type I isotherm curve [35], raising questions about its validity in this context. Tran *et al.* [26] assert that if β lies outside this range, the equation may fail to sufficiently explain the experimental data. Conversely, Chu *et al.* [35] suggest disregarding constraints on β, arguing that the equation is empirical and lacks a defined physical foundation, which renders the constant physically insignificant.

The other models are represented by increasing curves (Langmuir, Freundlich, and Sips) and a nearly constant line (Temkin), indicating that the solution obtained did not accurately depict a decreasing q_e curve. Consequently the adjustment may have been affected by the reduced magnitude of the q_e experimental values, resulting in a small error between calculated and experimental values, which reduces OF and creates a misleading impression that the adjustments were adequate.

The Langmuir model assumes a homogeneous adsorbent surface with energetically equivalent sites, where each one accommodates a single adsorbate molecule, leading to monolayer adsorption. It also predicts adsorbent saturation, which corresponds to a plateau in the q_e as a function of C_e curve. In contrast, the Freundlich model represents heterogeneous surface adsorbents, allowing for multilayer adsorption without predicting saturation. These two models have been combined to develop new empirical isotherm equations, such as Sips and Redlich-Peterson, which exhibit behaviors that approach either Langmuir or Freundlich characteristics based on their exponential constants. Specifically, the equations converge to the Langmuir model when β approaches to 1 and exhibit Freundlich behavior as the constant approaches zero [36].

As previously mentioned, the responses for the Langmuir, Freundlich, and Sips models were quite similar (as shown in Figure 4). However, Redlich-Peterson adjustment was able to predict the unusual adsorptive behavior, primarily due to the β value falling outside the 0-1 interval, indicating a possible deviation from both the Langmuir and Freundlich models.

Although the Redlich-Peterson fit was the most satisfactory, the observed behavior remains unusual and may be attributed to competition between DCF and other compounds for adsorption sites. Hilbrantd *et al.* [37] investigated adsorption in a multicomponent system containing phosphate and silicate, using ferric hydroxide as the adsorbent. They observed a mutual interference among ions during adsorption, obtaining a negative slope in the silicate adsorption isotherms, induced by phosphate presence.

Indeed, various potential interferents could contribute to the observed phenomenon, such as sodium ions naturally present in DCF, other ions from the pH adjustment solutions, or remnants in distilled water. However, identifying the interferent and comprehending the intensity of its effects might need further studies.

Adsorption kinetics

The adjustments to the PFO and PSO equations for the initial DCF concentrations are presented in Figure 5. Contrary to the graphs in Figure 3A, certain outliers were excluded from the curve to enhance the fitting to kinetic models.

For both models, the adjusted $q(t)$ values are similar, as the two curves practically overlap at all concentrations. Furthermore, the models predict a rapid establishment of equilibrium, as evidenced by the $q(t)$ for time intervals exceeding 5 min, which showed minimal variations and remained close to the estimated q_e. Additionally, the models correlate better with experimental data at the concentration of 2.5 mg L^{-1}.

The trends observed in Figure 5 are consistent with the parameters obtained for kinetic models. The ones considered relevant to the discussion are presented in the text, and all the obtained parameters are presented in Table S5 (Supplementary Material). The lowest OF and R^2 values closer to unity for PFO ($OF = 0.00033$, $R^2 = 0.9909$) and PSO ($OF = 0.00037$, $R^2 = 0.9897$) models were obtained at 2.5 mg L^{-1}. However, other concentrations did not exhibit appropriate adjustments for any kinetic model.
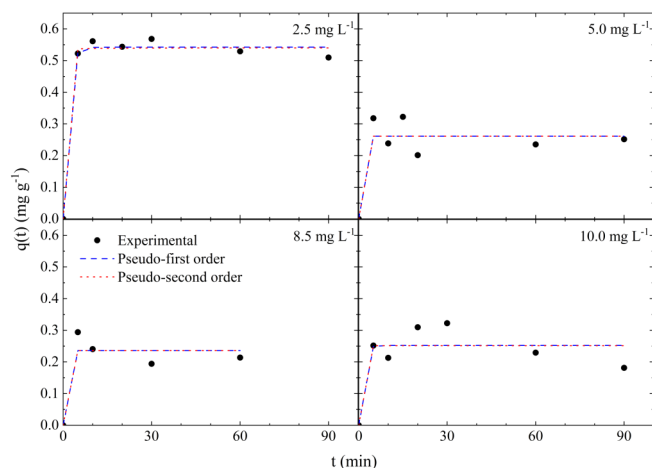

Figure 5. Experimental values of the adsorption capacity as a function of time and the fittings for the kinetic models at different initial DCF concentrations.

According to the PFO model, higher k_1 values are associated with smaller variations in $q(t)$ over time, resulting in q approaching q_e more rapidly. Moreover, k_1 can also reflect the speed at which the process reaches equilibrium, with higher values indicating a faster attainment of equilibrium [38]. Interestingly, for initial concentrations of 5.0 and 8.5 mg L^{-1}, which exhibited the highest k_1 values (3.5640 and 5.0536 min^{-1}, respectively), the calculated $q(t)$ at 5 min remained unchanged and equal to q_e. In contrast, for concentrations of 2.5 and 10.0 mg L^{-1}, with smaller k_1 values (0.6738 and 0.8921 min^{-1}, respectively), $q(t)$ slightly increased until 10 min before stabilizing at q_e. Thus, k_1 did not demonstrate a clear dependency on the initial adsorbate

concentration. Furthermore, the equilibrium showed minimal variations across the different concentrations, regardless of the calculated k_1 values.

The calculated k_2 constants for the PSO model exhibited a higher magnitude compared to other equation parameters. Consequently, $q(t)$ approaches q_e for all the time intervals starting from zero. This occurred across all initial concentrations, with the lowest k_2 value at 2.5 mg L^{-1} (61.136 g mg^{-1} min^{-1}), suggesting a more significant variation of $q(t)$ over time. While it was expected for the constant to decrease as the initial adsorbate concentration increased, the exact opposite occurred.

The decrease of k_1 and k_2 with rising initial concentration would indicate a slower establishment of equilibrium at higher initial adsorbate concentrations [38]. However, the film's divergent behavior could be attributed to the instability of results at concentrations exceeding 2.5 mg L^{-1}. It is plausible that precipitation might have occurred concomitantly with adsorption, interfering with the results, and limiting a more accurate analysis. Despite the instability, equilibrium time did not vary significantly across the concentrations, reiterating the film might possess a reduced adsorption capacity, which may lead to saturation at low adsorbate concentrations.

Additionally, the results of the experiments conducted at 2.5 mg L^{-1} (q_e = 0.5108 mg g^{-1}) are comparable to those reported by Rizzi *et al.* [34], who developed a chitosan adsorbent film for DCF removal. At an initial concentration of 7.5 × 10^{-6} mol L^{-1} (~ 2.38 mg L^{-1}), an initial pH of 5.0, and 50 mg of the film, they achieved a q_e of 0.55 mg g^{-1}, reaching equilibrium in 120 min. Although the adsorption performance appears adequate for a film configuration, the process still presents unidentified interferent factors. Therefore, a more comprehensive understanding of kinetics still requires further investigation, involving time intervals shorter than 5 min and at initial DCF concentrations lower than 2.5 mg L^{-1}.

Conclusion

Through this study, it was possible to access the film adsorptive performance for removing DCF from water. Moreover, possible interferences in the process were identified. The immersion in Extran® for glassware washing was linked to interference by the blank experiment results, and the film UV-Vis spectrum points to the feasibility of the film components release into the DCF solution. The contact with the film affected the DCF solution pH, reducing DCF solubility. The final pH was slightly higher than 4.0 (aligning with DCF pK_a), causing DCF precipitation for initial pH values below 8.0. Thus, the optimized initial pH was 8.0, associating better adsorptive performance with a higher final pH, to avoid precipitation. The initial concentration of 2.5 mg L^{-1} (the lowest value among those evaluated) led to the best performance (q_e = 0.511 mg g^{-1}, %R = 23.4%), reaching equilibrium within 90 min.

An increase in initial concentration did not enhance the adsorption capacity; instead, the results were similar across the

higher concentrations. Consequently, the Redlich-Peterson model provided a better representation of equilibrium (R^2 = 0.9767), while the other models failed to predict the decrease in q_e. Regarding kinetics, for the initial concentration of 2.5 mg L^{-1}, adsorption could be adequately described by both PFO and PSO models, as indicated by R^2 values close to unit and low *OF* values. Conversely, other concentrations exhibited more instability and did not yield adequate adjustments.

Although the performance is comparable to other film adsorbents, the lower adsorption capacity might be attributed to the dense film's reduced specific surface area, resulting in saturation at low adsorbate concentrations. A deeper understanding of the adsorptive behavior might involve investigating initial concentrations lower than 2.5 mg L^{-1}. This approach may allow for the observation of a more gradual evolution of the process and mitigate the effects of precipitation by working with DCF concentrations safely within the solubility limit.

Finally, this study provides important insights into the adsorptive characteristics of the film, despite its limited efficiency, contributing to a better understanding of its performance in membrane separation processes. To enhance its suitability for real water treatment applications, further improvements are needed, potentially through the incorporation of additives such as lignocellulosic biomass. Additionally, focusing on regeneration, reusability, and performance under actual wastewater treatment conditions will aid in developing a viable environmental remediation solution.

Authors Contribution

J. Z. Merck: Conceptualization, Methodology, Validation, Formal Analysis, Investigation, Writing - Original Draft; C. S. Raota: Conceptualization, Methodology, Validation, Writing - Review & Editing, Visualization; J. Duarte: Methodology, Validation; C. Baldasso: Resources; M. Giovanela: Writing - Review & Editing; J. S. Crespo: Conceptualization, Resources, Writing - Review & Editing, Visualization, Supervision, Project Administration, Funding Acquisition. All authors have approved the final version of the manuscript.

Conflicts of Interest

The authors declare that they have no known competing financial interests or personal relationships that could have appeared to influence the work reported in this paper.

Supplementary Material

Supplementary material associated with this article can be found online at: https://doi.org/10.18226/23185279.e241305.

References

[1] L. Qalyoubi, A. Al-Othman, S. Al-Asheh, Recent progress and challenges on adsorptive membranes for the removal of pollutants from wastewater. Part I: fundamentals and classification of membranes. *Case Studies in Chemical and Environmental Engineering*, vol 3, pp. 100086, 2021. DOI: http://dx.doi.org/10.1016/j.cscee.2021.100086.

[2] J. O. Ighalo, A. G. Adeniyi, Mitigation of diclofenac pollution in aqueous media by adsorption. *Chembioeng Reviews*, vol 7, pp. 50-64, 2020. DOI: https://doi.org/10.1002/cben.201900020.

[3] T. B. Veras, A. L. R. Paiva, M. M. M. B. Duarte, D. C. Napoleão, J. J. S. P. Cabral, Analysis of the presence of anti-inflammatories drugs in surface water: a case study in beberibe river - PE, Brazil. *Chemosphere*, vol 222, pp. 961-969, 2019. DOI: http://dx.doi.org/10.1016/j.chemosphere.2019.01.167.

[4] L. Lonappan, S. K. Brar, R. K. Das, M. Verma, R. Y. Surampalli, Diclofenac and its transformation products: environmental occurrence and toxicity - a review. *Environment International*, vol 96, pp. 127-138, 2016. DOI: http://dx.doi.org/10.1016/j.envint.2016.09.014.

[5] C. Eades, C. P. Waring, The effects of diclofenac on the physiology of the green shore crab *Carcinus maenas*. *Marine Environmental Research*, vol 69, pp. S46-S48, 2010. DOI: http://dx.doi.org/10.1016/j.marenvres.2009.11.001.

[6] S. A. S. Melo, A. G. Trovó, I. R. Bautitz, R. F. P. Nogueira, Degradação de fármacos residuais por processos oxidativos avançados. *Química Nova*, vol 32, pp. 188-197, 2009. DOI: http://dx.doi.org/10.1590/s0100-40422009000100034;.

[7] Y. Zhang, S. U. Geißen, C. Gal, Carbamazepine and diclofenac: removal in wastewater treatment plants and occurrence in water bodies. *Chemosphere*, vol 73, pp. 1151-1161, 2008. DOI: http://dx.doi.org/10.1016/j.chemosphere.2008.07.086.

[8] A. Khalidi-Idrissi, A. Madinzi, A. Anouzla, A. Pala, L. Mouhir, Y. Kadmi, S. Souabi, Recent advances in the biological treatment of wastewater rich in emerging pollutants produced by pharmaceutical industrial discharges. *International Journal of Environmental Science and Technology*, vol 20, pp. 11719-11740, 2023. DOI: http://dx.doi.org/10.1007/s13762-023-04867-z.

[9] S. F. Aquino, E. M. F. Brandt, C. A. L. Chernicharo, Remoção de fármacos e desreguladores endócrinos em estações de tratamento de esgoto: revisão da literatura. *Engenharia Sanitaria e Ambiental*, vol 18, pp. 187-204, 2013. DOI: http://dx.doi.org/10.1590/s1413-41522013000300002.

[10] R. Singh, V. S. K. Yadav, M. K. Purkait, Cu_2O photocatalyst modified antifouling polysulfone mixed matrix membrane for ultrafiltration of protein and visible light driven photocatalytic pharmaceutical removal. *Separation And Purification Technology*, vol 212, pp. 191-204, 2019. DOI: http://dx.doi.org/10.1016/j.seppur.2018.11.029.

[11] K. P. M. Licona, L. R. O. Geaquinto, J. V. Nicolini, N. G. Figueiredo, S. C. Chiapetta, A. C. Habert, L. Yokoyama, Assessing potential of nanofiltration and reverse osmosis for removal of toxic pharmaceuticals from water. *Journal of Water Process Engineering*, vol 25, pp. 195-204, 2018. DOI: http://dx.doi.org/10.1016/j.jwpe.2018.08.002.

[12] M. S. Shamsudin, S. F. Azha, L. Sellaoui, M. Badawi, A. Bonilla-Petriciolet, S. Ismail, Performance and interactions of diclofenac adsorption using alginate/carbon-based films: experimental investigation and statistical physics modelling. *Chemical Engineering Journal*, vol 428, pp. 131929, 2022. DOI: http://dx.doi.org/10.1016/j.cej.2021.131929.

[13] P.V. Viotti, W. M. Moreira, O. A. A. Santos, R. Bergamasco, A. M. S. Vieira, M. F. Vieira, Diclofenac removal from water by adsorption on *Moringa oleifera* pods and activated carbon: mechanism, kinetic and equilibrium study. *Journal of Cleaner Production*, vol 219, pp. 809-817, 2019. DOI: http://dx.doi.org/10.1016/j.jclepro.2019.02.129.

[14] A. Bonilla-Petriciolet, D. I. Mendoza-Castillo, H. E. Reynelávila. Adsorption processes for water treatment and purification. Switzerland: Springer, 2017.

[15] L. Qalyoubi, A. Al-Othman, S. Al-Asheh, Recent progress and challenges of adsorptive membranes for the removal of pollutants from wastewater. Part II: environmental applications. *Case Studies in Chemical and Environmental Engineering*, vol 3, pp. 100102, 2021. DOI: http://dx.doi.org/10.1016/j.cscee.2021.100102.

[16] M. D. Raicopol, C. Andronescu, S. I. Voicu, E. Vasile, A. M. Pandele, Cellulose acetate/layered double hydroxide adsorptive membranes for efficient removal of pharmaceutical environmental contaminants. *Carbohydrate Polymers*, vol 214, pp. 204-212, 2019. DOI: http://dx.doi.org/10.1016/j.carbpol.2019.03.042.

[17] R. Nagarkar, J. Patel, Polyvinyl alcohol: a comprehensive study. *Acta Scientific Pharmaceutical Sciences*, vol 3, pp. 34-44, 2019.

[18] G. Göksen, M. J. Fabra, A. Pérez-Cataluña, H. I. Ekiz, G. Sanchez, Biodegradable active food packaging structures based on hybrid cross-linked electro spun polyvinyl alcohol fibers containing essential oils and their application in the preservation of chicken breast fillets. *Food Packaging and Shelf Life*, vol 27, pp. 100613, 2021. DOI: http://dx.doi.org/10.1016/j.fpsl.2020.100613.

[19] J. Perez-Calderon, D. A. Marin-Silva, N. Zaritzky, Eco-friendly PVA-chitosan adsorbent films for the removal of azo dye acid orange 7: physical cross-linking, adsorption process, and reuse of the material. *Advanced Industrial and Engineering Polymer Research*, vol 6, pp. 239-254, 2023. DOI: http://dx.doi.org/10.1016/j.aiepr.2022.12.001.

[20] S. Shang, K. L. Chiu, S. Jiang, Synthesis of immobilized poly(vinyl alcohol)/cyclodextrin eco-adsorbent and its application for the removal of ibuprofen from pharmaceutical sewage. *Journal of Applied Polymer Science*, vol 134, pp. 1-7, 2017. DOI: http://dx.doi.org/10.1002/app.44861.

[21] C. F. Mok, Y. C. Ching, F. Muhamad, N. A. A. Osman, N. D. Hai, C. R. C. Hassan, Adsorption of dyes using poly (vinyl alcohol) (PVA) and PVA-based polymer composite adsorbents: a review. *Journal of Polymers and the Environment*, vol 28, pp. 775-793, 2020. DOI: http://dx.doi.org/10.1007/s10924-020-01656-4.

[22] C. S. Raota, J. S. Crespo, C. Baldasso, M. Giovanela, Development of a green polymeric membrane for sodium diclofenac removal from aqueous solutions. *Membranes*, vol 13, pp. 662, 2023. DOI: https://doi.org/10.3390/membranes13070662.

[23] C. S. Raota, J. Duarte, J. S. Crespo, C. Baldasso, M. Giovanela, Process optimization for the removal of sodium diclofenac from water using a green polymeric membrane. *Journal of Environmental Chemical Engineering*, vol 12, pp. 113237, 2024. DOI: http://dx.doi.org/10.1016/j.jece.2024.113237.

[24] C. S. Raota, A. F. Cerbaro, M. Salvador, A. P. L. Delamare, S. Echeverrigaray, J. S. Crespo, T. B. Silva, M. Giovanela, Green synthesis of silver nanoparticles using an extract of Ives cultivar (*Vitis labrusca*) pomace: characterization and application in wastewater disinfection. *Journal of Environmental Chemical Engineering*, vol 7, pp. 103383, 2019. DOI: http://dx.doi.org/10.1016/j.jece.2019.103383.

[25] Y. Lu, L. Fan, L. Y. Yang, F. Huang, X. K. Ouyang, PEI-modified core-shell/bead-like amino silica enhanced poly (vinyl alcohol)/chitosan for diclofenac sodium efficient adsorption. *Carbohydrate Polymers*, vol 229, pp. 115459, 2020. DOI: http://dx.doi.org/10.1016/j.carbpol.2019.115459.

[26] H. N. Tran, S. J. You, A. Hosseini-Bandegharaei, H. P. Chao, Mistakes and inconsistencies regarding adsorption of contaminants from aqueous solutions: a critical review. *Water Research*, vol 120, pp. 88-116, 2017. DOI: http://dx.doi.org/10.1016/j.watres.2017.04.014.

[27] S. Pandit, S. Kundu, Optical and structural behaviors of crosslinked polyvinyl alcohol thin films. DAE *Solid State Physics Symposium*, vol 1942, pp. 080029-1 - 080029-4, 2018. DOI: https://doi.org/10.1063/1.5028863.

[28] E. Rusu, A. Airinei, V. Barboiu, D. Timpu, Some characteristics of poly(vinyl alcohol) with azido aromatic groups. *Journal of Optoelectronics and Advanced Materials*, vol 9, pp. 1044-1047, 2007.

[29] N. Jamil, H. Husin, A. W. Alfida, Z. Aman, Z. Hassan, Characterization and preparation of polyvinyl alcohol (PVA) as inhibitor in formation of hydrates. *International Journal of Current Research in Science Engineering & Technology*, vol 1, pp. 578-584, 2018. DOI: http://dx.doi.org/10.30967/ijcrset.1.s1.2018.578-584.

[30] S. Krishnaswamy, V. Ragupathi, S. Raman, P. Panigrahi, G. S. Nagarajan, Study of optical and electrical property of NaI-doped PPy thin film with excellent photocatalytic property at visible light. *Polymer Bulletin*, vol 76, pp. 5213-5231, 2018. DOI: https://doi.org/10.1007/s00289-018-2650-1.

[31] S. Mohan, Y. Singh, D. K. Verma, S. H. Hasan, Synthesis of CuO nanoparticles through green route using Citrus limon juice and its application as nanosorbent for Cr (VI) remediation: Process optimization with RSM and ANN-GA based model. *Process Safety and Environmental Protection*, vol 96, pp. 156-166, 2015. DOI: https://doi.org/10.1016/j.psep.2015.05.005.

[32] S. K. Bajpai, M. Bhowmik, Adsorption of diclofenac sodium from aqueous solution using polyaniline as a potential sorbent. I. Kinetic studies. *Journal of Applied Polymer Science*, vol 117, pp. 3615-3622, 2010. DOI: https://doi.org/10.1002/app.32263.

[33] M. Antunes, V. I. Esteves, R. Guégan, J. S. Crespo, A. N. Fernandes, M. Giovanela. Removal of diclofenac sodium from aqueous solution by Isabel grape bagasse. *Chemical Engineering Journal*, vol 192, pp. 114-121, 2012. DOI: http://dx.doi.org/10.1016/j.cej.2012.03.062.

[34] V. Rizzi, F. Romanazzi, J. Gubitosa, P. Fini, R. Romita, A. Agostiano, A. Petrella, P. Cosma, Chitosan film as eco-friendly and recyclable bio-adsorbent to remove/recover diclofenac, ketoprofen, and their mixture from wastewater. *Biomolecules*, vol 9, pp. 571, 2019. DOI: http://dx.doi.org/10.3390/biom9100571.

[35] K. H. Chu, M. A. Hashim, Y. T. C. Santos, J. Debord, M. Harel, J. C. Bollinger, The Redlich–Peterson isotherm for aqueous phase adsorption: pitfalls in data analysis and interpretation. *Chemical Engineering Science*, vol 285, pp. 119573, 2024. DOI: http://dx.doi.org/10.1016/j.ces.2023.119573.

[36] K. Y. Foo, B. H. Hameed, Insights into the modeling of adsorption isotherm systems. *Chemical Engineering Journal*, vol 156, pp. 2-10, 2010. DOI: http://dx.doi.org/10.1016/j.cej.2009.09.013.

[37] I. Hilbrandt, V. Lehmann, F. Zietzschmann, A. S. Ruhlc, M. Jekel, Quantification and isotherm modelling of competitive phosphate and silicate adsorption onto micro-sized granular ferric hydroxide. *RSC Advances*, vol 9, pp. 23642-23651, 2019. DOI: https://doi.org/10.1039/c9ra04865k.

[38] W. Plazinski, W. Rudzinski, A. Plazinska, Theoretical models of sorption kinetics including a surface reaction mechanism: a review. *Advances In Colloid and Interface Science*, vol 152, pp. 2-13, 2009. DOI: http://dx.doi.org/10.1016/j.cis.2009.07.009.